the primary source responsible for the interface states, it is not difficult to conceive that a very basic change in the mode of oxidant diffusion could bring about an appreciable change in the interface state density. As the oxidation of silicon proceeds inward, the conditions prevailing during the growth of the last monolayer determine the interface properties.

Sakurai and Sugano[10] have carried out a theoretical calculation of the $Si\text{-}SiO_2$ interface state density distribution. Their calculations indicated Si dangling bonds generate interface states in the midgap region, O–vacancy and Si–Si weak bonds generate states in the upper band-gap region, and Si–O weak bonds generate states in the lower band-gap region. Furthermore, the energy location of the trap state was found to vary with the bonding parameters such as bond lengths and bond angles. The shift in E_{peak} observed by us could reflect variations in the bonding parameters, brought about by changes in the oxidation process.

In conclusion, an interesting observation of our experimental investigation concerns the interface state density versus oxide thickness profile, which appears to go through a valley followed by a peak, instead of being a monotonically decreasing one. The valley/peak feature in the profile may reflect the transition in the diffusion of the oxidizing species from the field-aided mode to the field-free mode.

This work has been carried out under a cooperative research project between Indian Institute of Technology, Kanpur and The Pennsylvania State University, University Park, supprted by National Science Foundation, USA, grants INT-8012203 and DAR-8010854, respectively.

[1]R. L. Narasimhan, D. Shanker, and S. Kar (unpublished).
[2]S. Kar and S. Varma, J. Appl. Phys. **54**, 1988 (1983).
[3]S. Kar, S. Varma, P. Saraswat, and S. Ashok, J. Appl. Phys. **53**, 7039 (1982).
[4]S. Kar and S. Varma, J. Appl. Phys. **58**, 4256 (1985).
[5]N. M. Johnson, D. K. Biegelsen, and M. D. Moyer, in *Proceedings of International Topical Conference on the Physics of SiO_2 and its Interfaces*, edited by G. Lucovsky, S. T. Pantelides, and F. L. Galeener (Pergamon, New York, 1980), p. 331.
[6]E. H. Poindexter, G. J. Gerardi, M.-E. Rueckel, P. J. Caplan, N. M. Johnson, and D. K. Biegelsen, J. Appl. Phys. **56**, 2844 (1984).
[7]B. E. Deal and A. S. Grove, J. Appl. Phys. **36**, 3770 (1965).
[8]B. E. Deal, M. Sklar, A. S. Grove, and E. H. Snow, J. Electrochem. Soc. **114**, 266 (1967).
[9]N. Cabrera and N. F. Mott, Rep. Prog. Phys. **12**, 163 (1948).
[10]T. Sakurai and T. Sugano, J. Appl. Phys. **52**, 2889 (1981).

Effects of GaAs/AlAs superlattice buffer layers on selective area regrowth for GaAs/AlGaAs self-aligned structure lasers

Susumu Noda, Kenzo Fujiwara, and Takashi Nakayama
Central Research Laboratory, Mitsubishi Electric Corporation, 8-1-1 Tsukaguchi-honmachi, Amagasaki, Hyogo 661, Japan

(Received 14 June 1985; accepted for publication 24 September 1985)

The effects of GaAs/AlAs superlattice buffer layers on selective area regrowth by molecular beam epitaxy were investigated for self-aligned structure lasers. It is demonstrated that the superlattice buffer layer is an effective means to obtain a smoother interface with reduced alloy clustering, from which the threshold current was reduced and stable single transverse mode operation was obtained.

Recently, molecular beam epitaxy (MBE) has attracted a considerable interest as an excellent epitaxial growth technique for optoelectronic devices.[1] A large uniform epitaxial layer (thickness fluctuation less than $\pm 5\%$) over a 3-in. wafer grown by MBE is a great advantage for mass production as compared with conventional liquid phase epitaxy (LPE). The MBE process offers a more significant capability, i.e., the controlled ability to fabricate superfine heterostructures of designed thickness, composition, and doping profiles. Fabrication of sophisticated devices such as a multiple quantum well (MQW) laser[2] and a high electron mobility transistor (HEMT)[3] makes use of this advantage. In spite of its importance for device applications, however, the epitaxial growth over preferentially etched channels has not been well investigated. Such growth is indispensable for fabricating transverse mode controlled lasers[4–6] as well as integrated optoelectronic circuits (IOEC's).

In this letter, the effects of GaAs/AlAs superlattice (SL) buffer layers on selective area MBE growth are reported for the first time. We have studied these effects for the case of the GaAs/AlGaAs self-aligned structure (SAS) lasers, which require regrowth over a preferentially etched channel to obtain the lateral confinement.

Figure 1 shows a schematic diagram of the GaAs/AlGaAs SAS laser studied in this work. Both current and light parallel to the junction are confined in the stripe by the *n*-GaAs antiguiding layer. The SAS lasers were fabricated by a two-step MBE growth technique using a Varian Gen II system. The substrate temperature was 630 °C during growth. In the first step, seven layers of (1) *n*-GaAs (Si doped, 2×10^{18} cm^{-3}), 0.2 μm; (2) *n*-$Al_{0.3}Ga_{0.7}As$ (Si doped, 5×10^{17} cm^{-3}), 1.7 μm; (3) undoped GaAs, 0.11 μm; (4) *p*-$Al_{0.3}Ga_{0.7}As$ (Be doped, 5×10^{18} cm^{-3}), 0.3 μm; (5) *n*-GaAs (Si doped, 1×10^{18} cm^{-3}), 0.74 μm; (6) *n*-$Al_{0.3}Ga_{0.7}As$ (Si

 © 1985 American Institute of Physics

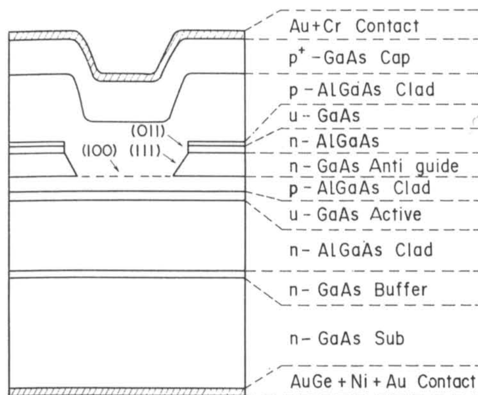

FIG. 1. Schematic diagram of the self-aligned structure (SAS) laser, where the (100), (111), and (011) facets were in the groove.

doped, 1×10^{18} cm^{-3}), 0.20 μm; (7) undoped GaAs, 500 Å were sequentially grown on (100) oriented n-GaAs substrates (Si doped, 2×10^{18} cm^{-3}). After the first growth, a silicon nitride SiN_x film was deposited by plasma-assisted chemical vapor deposition, and 6 μm window stripes (parallel to [01$\bar{1}$] direction) were formed by conventional photolithography and dry etching. Then the wafer was successively etched through the SiN_x mask by $9H_2SO_4$:$1H_2O_2$:$1H_2O$ solution at 5 °C and $30H_2O_2$:$1NH_4OH$ solution at room temperature down to the fifth n-GaAs antiguiding layer. After the SiN_x was removed, the remaining $Al_{0.3}Ga_{0.7}As$ eaves were removed by a supersonic microcleavage method. The (100), (111), and (011) facets were formed in the groove. Here we have the (011) facet, which is a very steep facet. The final width of the channel stripe was about 9 μm.

After the formation of the groove, a second MBE growth was done under the similar growth condition. At this stage, the wafer was divided into two parts. For one part of the wafer, two layers of 1.4 μm p-$Al_{0.3}Ga_{0.7}As$ (Be doped, 5×10^{18} cm^{-3}) and 0.6 μm p-GaAs (Be doped, 1×10^{19} cm^{-3}) were grown. For the other part, a GaAs/AlAs superlattice buffer layer was additionally inserted at the regrown interface. The SL buffer layer was composed of 30 pairs of GaAs ($l_z\sim35$ Å) and AlAs ($l_b\sim23$ Å) layers (Be doped, 5×10^{18} cm^{-3}). After the second growth, ohmic contacts to the diodes were made by evaporating Cr-Au on the p side and AuGe-Ni-Au on the n side, followed by sintering in an H_2 atmosphere.

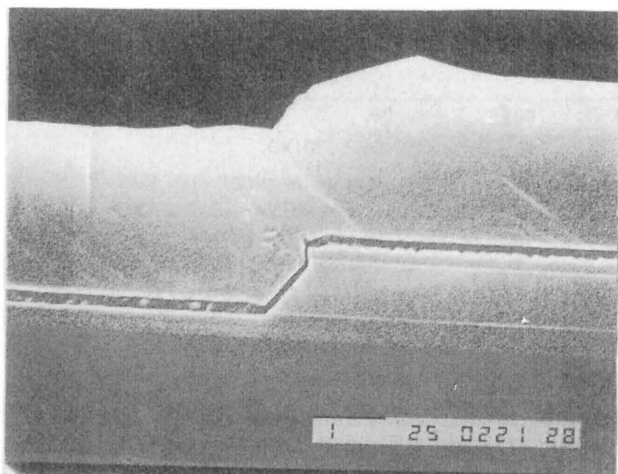

(a)

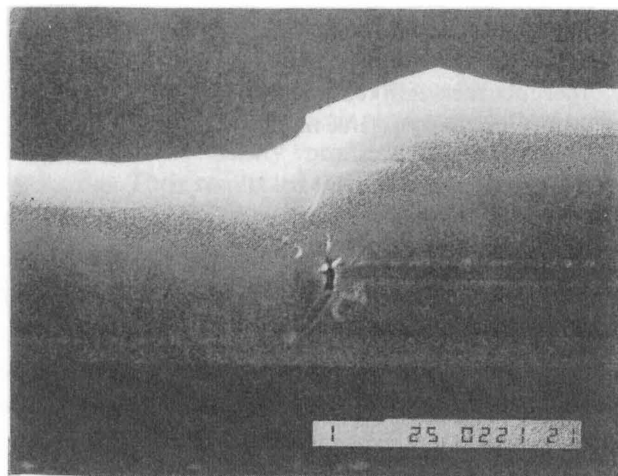

(b)

1 μm

FIG. 2. Scanning electron microscopic pictures of the SAS lasers: (a) with superlattice buffer layer; (b) without superlattice buffer layer.

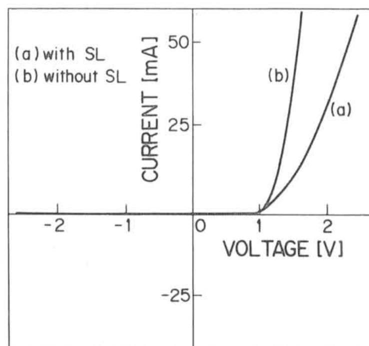

FIG. 3. Current-voltage characteristics of the SAS lasers: (a) with superlattice buffer layer; (b) without superlattice buffer layer.

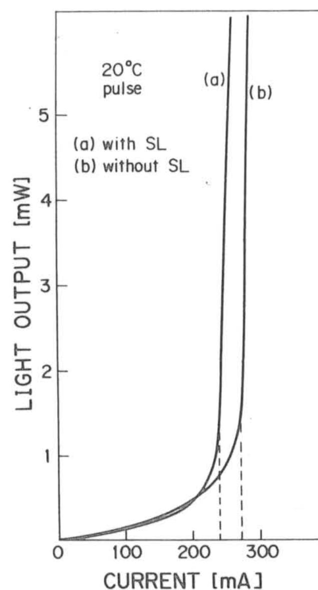

FIG. 4. Current-light output characteristics of the SAS lasers: (a) with superlattice buffer layer; (b) without superlattice buffer layer.

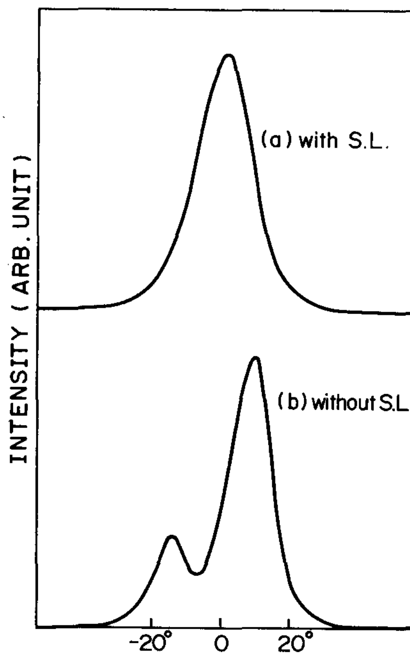

FIG. 5. Far-field patterns of the SAS lasers at 5 mW: (a) with superlattice buffer layer; (b) without superlattice buffer layer.

Cleaved and etched cross-sectional views of the lasers with and without SL buffer layer were shown in Figs. 2(a) and 2(b), respectively. The higher contrast at the interface in Fig. 2(a) is due to the deep etching of the SL by the stain etchant. The regrown interface with the SL is much smoother than that without SL, especially on the (011) facet. The disorder on the (011) facet without SL is caused by the following reason. The (011) facet is too steep to obtain uniform irradiation of the molecular beam from the source, so that alloy clustering occurred and crystal defects such as stacking faults might be introduced into the overgrown layer. On the other hand, in case of the laser with an SL buffer layer, a fairly smooth interface was obtained even on the (011) facet, since the alloy clustering was suppressed by the binary SL and the stacking faults might be eliminated by the flattening effect due to the slight difference of lattice constants between GaAs and AlAs.[7]

Typical *I-V* characteristics of the lasers with and without SL buffer layers are shown in Figs. 3(a) and 3(b), respectively. The built-in voltage of each laser was about 1 V. However, the resistance of the laser with the SL is 2.5 times higher than that without the SL, which may be caused by the unoptimized values of l_z and l_b.

Figure 4 shows typical *I-L* characteristics of the lasers with and without SL buffer layers in pulsed operation (5 μs pulse width, 1 ms duration) at room temperature. The cavity length of each laser was 330μm. The threshold current I_{th} of the laser with SL was 238 mA, while that of the laser without SL was 270 mA. It was found that I_{th} of the lasers with SL was always 8–12% less than that without SL in spite of its higher series resistance. This result indicates that the optical loss was reduced in the grooved channel due to the improved interface by the SL buffer layer. It is expected that the device characteristics can be further improved by optimizing the designed parameters of the SL buffer layer.

We also studied the transverse mode characteristics of the lasers. Figure 5 shows the far-field patterns parallel to the junction at 5 mW. The laser with a SL buffer layer was in single transverse mode whereas the laser without a SL was in transverse multimode. This is due to the following reason. The laser without a SL has compositional fluctuations due to alloy clustering at the regrown interface as shown in Fig. 2(b), which caused an abrupt refractive index change, and the electric field is strongly confined in the relatively wide ($\sim$9 μm) stripe, thus higher order mode appeared. On the other hand, the laser with a SL has a smoother interface at the groove as shown in Fig. 2(a); therefore, a single transverse mode was obtained.

In summary, the effects of GaAs/AlAs superlattice buffer layers on selective area MBE growth were investigated for the case of the SAS lasers. A very smooth interface was obtained from the SL buffer layer, so that the threshold current was reduced and stable single transverse mode operation was obtained.

The authors would like to thank K. Kyuma, K. Mitsunaga, and K. Kojima for continuous encouragement and helpful discussions.

[1]W. T. Tsang, IEEE J. Quantum Electron. **QE-20**, 1119 (1984).
[2]N. Holonyak, Jr., R. M. Kolbas, R. D. Dupuis, and P. D. Dupkus, IEEE J. Quantum Electron **QE-16**, 170 (1980).
[3]S. Hiyamizu and T. Mimura, J. Cryst. Growth **56**, 455 (1982).
[4]T. P. Lee and A. Y. Cho, Appl. Phys. Lett. **29**, 164 (1976).
[5]A. Y. Cho, Jpn. J. Appl. Phys. **16**, Suppl. 16-1, 435 (1977).
[6]H. Tanaka, M. Mushiage, Y. Ishida, and H. Fukada, Jpn. J. Appl. Phys. **24**, L89 (1985).
[7]P. M. Petroff, R. C. Miller, A. C. Gossard, and W. Wiegman, Appl. Phys. Lett. **44**, 217 (1984).